Available online at www.sciencedirect.com

SciVerse ScienceDirect

Ceramics International 38 (2012) 6849–6856

CERAMICS INTERNATIONAL

www.elsevier.com/locate/ceramint

In vitro bonelike apatite formation on magnetite nanoparticles after a calcium silicate treatment: Preparation, characterization and hemolysis studies

E.M. Múzquiz-Ramos[a,b,*], D.A. Cortés-Hernández[a], J.C. Escobedo-Bocardo[a], A. Zugasti-Cruz[b]

[a]*CINVESTAV IPN-Unidad Saltillo, Carretera Saltillo-Mty, Km 13, Apdo. Postal. 663, C.P. 25000, Saltillo, Coah, Mexico*
[b]*Facultad de Ciencias Químicas, Universidad Autónoma de Coahuila, Blvd. V. Carranza y José Cárdenas, Apdo. Postal 935, C.P. 25280, Saltillo, Coah, Mexico*

Received 25 April 2012; received in revised form 11 May 2012; accepted 25 May 2012
Available online 7 June 2012

Abstract

Bioactive magnetite nanoparticles were prepared successfully by coating magnetite nanoparticles with $CaSiO_3$ followed by their immersion in simulated body fluid. The Fe_3O_4 nanoparticles (5–10 nm) were synthesized by a co-precipitation technique. In order to prepare core–shell nanocomposites, the nanoparticles were soaked for 1 h in a calcium silicate solution that had been aged for 24 h before using it. The samples were dried in air and then immersed in SBF at 37 °C for 1, 3 and 7 days. The analyses of the samples after the biomimetic process revealed the formation of a bonelike apatite layer on all the samples tested and not a significant change was observed on their original magnetic behavior. Hemolysis test, evaluated as release of hemoglobin, revealed that all the samples showed no hemolytic effects up to 3 mg/ml, indicating no damage of the red blood cell membranes. These bioactive, hemocompatible and superparamagnetic particles may be potential materials for bone cancer treatment by hyperthermia.

Keywords: Magnetite nanoparticles; Calcium silicate; Biomimetic process; Hyperthermia

1. Introduction

Magnetic particles ranging from the nanometer to micrometer scale are being used in an increasing number of medical applications [1]. Because of their dimensions, nanosized particles have properties that are not characteristic of either the atom or the bulk counterparts. In the last decade, a large number of investigations with several types of iron oxides have been carried out in order to evaluate their use in several biomedical applications, such as hyperthermia, cell labeling, tissue repair, magnetic resonance imaging and drug delivery. For these applications, in order for the particles to be effective, they must combine certain properties. For example, to produce an effective magnetic enrichment, they should possess a high magnetic susceptibility. Moreover, their size has to be smaller than a critical size (about 15 nm, depending on the composition) so that the particles would consist of a single magnetic domain, i.e. the particles exhibit the so-called superparamagnetism [2].

Several materials that generate heat by hysteresis loss have been developed [3] and the magnetite nanoparticles are highly suitable for hyperthermia because of their strong ferrimagnetic behavior, which leads to a relatively high magnetic saturation and biocompatibility [4]. The sub-10 nm magnetite nanoparticles exhibit superparamagnetic behavior due to the fact that each particle can be considered as a single magnetic domain [5] and this property is particularly interesting, as they do not retain

*Corresponding autor at: CINVESTAV IPN-Unidad Saltillo, Carretera Saltillo-Mty, Km 13, Apdo. Postal. 663, C.P. 25000, Saltillo, Coah, Mexico. Tel.: +52 844 4389600x9683; fax: +52 844 4389610.
E-mail address: emuzquiz@uadec.edu.mx (E.M. Múzquiz-Ramos).

0272-8842/$36.00
http://dx.doi.org/10.1016/j.ceramint.2012.05.085

any magnetism after the removal of the applied magnetic field [6].

Hyperthermia is a promising approach to cancer therapy. It is based on the heating of the target tissue to slightly above body temperature. This can generally reduce the viability of cancer cells and increasing their sensitivity to chemotherapy and radiation. This technology is based on the fact that magnetic particles produce heat through various kinds of energy losses during application of an external AC magnetic field [7]. Cancer cells generally perish at around 43 °C because their oxygen supply via the blood vessels is not sufficient, whereas normal cells are not damaged at even higher temperatures [8].

Magnetite nanoparticles under an alternating magnetic field are expected to be useful thermoseeds in hyperthermic cancer treatment since they can be targeted and confined into the cancer site without damaging normal cells. All biomedical and bioengineering applications require that these ferrites must have not only high magnetization values and narrow particle size distribution, but they have also to be non-toxic and biocompatible [9].

The surfaces of iron-oxide nanoparticles are, in chemical terms, relatively inert, and there are only a limited number of molecules that can be covalently bonded to the particles surface. This is the reason why certain changes to the surfaces must be performed, such as functionalization. Apart from enabling the selective binding of different bioactive molecules, the functionalized nanoparticles must exhibit appropriate magnetic properties; they have to be non-toxic, hydrophilic and biocompatible, and they have to remain stable in aqueous colloidal suspensions [10]. Design and synthesis of discreet magnetic nanoparticles, where each particle is coated with a biocompatible molecule, are keys for obtaining magnetic materials for biotechnological applications [11].

Bonelike apatite coatings obtained by biomimetic methods bond to living bone. The biomimetic methods consist mainly in the deposition of a bonelike apatite layer on the substrate by immersing samples in simulated body fluids (SBF, 1.4 SBF, 1.5 SBF and 5 SBF) for different periods of time. As reported previously [12], the formation of apatite was enhanced using a re-immersion method in which the SBF was periodically replaced to maintain a high ionic concentration. Moreover, if a wollastonite ($CaSiO_3$) bed is used as a calcium ion supplier during the first phase of immersion, the apatite nucleation is more effective [13,14].

Bioactivity can be induced on bioinert surfaces either by the formation of functional groups or by the formation of thin ceramic phases that have the potential to form functional groups on exposure to a body environment [15]. Some calcium silicates are bioactive materials that form an apatite layer on their surface when they are in contact with real or SBF. The apatite formation is mainly due to the Ca^{2+} that is released into the SBF from wollastonite leading to the increase of the supersaturation degree of the fluid with respect to apatite by increasing pH [16]. At the beginning of the reaction an ionic exchange of Ca^{2+} for H^+ takes place on the wollastonite surface. The ionic exchange transforms the wollastonite crystals into an amorphous silica phase and increases the calcium concentration and the pH of the surrounding SBF. Under these conditions, apatite nucleation on the surface and the simultaneous solution of the amorphous silica take place [17,18]. In a previous work [19] we have showed that it is possible to form a bonelike apatite layer on magnetite nanoparticles after a week of biomimetic treatment using SBF and wollastonite.

It has been reported that the incorporation of silanol (Si–OH) groups into the chitosan microparticles leads to bone-bonding ability to the microparticles when they are immersed in SBF, accelerating the tissue integration, which leads to the unique strength of such interfaces [20]. However, this technique has not been applied to the bioactivation of magnetite nanoparticles.

The aim of this work was to prepare magnetite nanoparticles coated with a bonelike apatite layer by treating the magnetite nanoparticles in a calcium silicate solution followed by their immersion in SBF. The coated particles may be potential thermoseeds for bone cancer treatment.

2. Material and methods

2.1. Preparation of magnetite nanoparticles

Magnetite nanoparticles were synthesized by a chemical co-precipitation technique [21] using 0.1 M separate solutions of the following reagent grade chemicals: $FeCl_3 \cdot 6H_2O$ (Sigma-Aldrich) and $FeCl_2 \cdot 4H_2O$ (Sigma-Aldrich). These solutions were prepared by dissolving appropriate amounts of the starting chemicals in distilled water. Appropriate amounts of solutions were mixed in a Pyrex baker using a mechanical stirrer (around 1000 rpm) to obtain a Fe^{+2}:Fe^{+3} ratio of 2:3 while heating on a hot plate. When 70 °C of temperature was reached, the stirring velocity was increased up to 5000 rpm to produce an effective reaction and then NH_4OH (Sigma-Aldrich) at 10% was promptly added. A black color, characteristic of the precipitated nanoparticles, was observed. The precipitate was washed several times with distilled water to eliminate as much as possible the residual chlorides. The magnetite particles were dried in air at room temperature.

2.2. Calcium silicate solution treatment

The solution was prepared as reported [20]: TEOS: $Si(OC_2H_5)_4$(Sigma-Aldrich), deionized water, (C_2H_5OH) (Sigma-Aldrich), 1 M aqueous HCl solution and $CaCl_2$ (Sigma-Aldrich) were mixed for 10 min at 0 °C in order to prepare a calcium silicate solution with a molar ratio of $TEOS/H_2O/C_2H_5OH/HCl/CaCl_2$ of 1.0/4.0/4.0/0.014/0.20. The solution was aged for 24 h before using it. The nanoparticles were soaked in the aged calcium silicate solution at 36 °C and 120 rpm for 60 min. The final

product was obtained by magnetic separation and then dried in air at room temperature.

2.3. Biomimetic treatment

For the biomimetic process an SBF with an ionic concentration nearly equal to that of human blood plasma was used [22]. The solution was prepared by dissolving reagent-grade chemicals (Sigma-Aldrich) of NaCl, $NaHCO_3$, KCl, K_2HPO_4 $3H_2O$, $MgCl_2$ $6H_2O$, $CaCl_2$ $2H_2O$ and Na_2SO_4 in deionized water and buffered to pH 7.4 with tris(hydroxymethyl)-aminomethane and 1.0 N HCl at 36.5 °C [16]. The calcium silicate-coated magnetite nanoparticles were immersed in SBF at a solid/liquid weight ratio of 0.5 g/150 ml at 36.5 °C for three different periods: 1, 3 and 7 days. At the end of the immersion periods, the magnetite powder was removed from the flasks, washed gently with deionized water and dried at room temperature.

2.4. Characterization

The surfaces of the magnetite nanoparticles before and after the solution treatment and the subsequent biomimetic treatment were analyzed by scanning electron microscopy (SEM) (JSM 6300, Jeol, Japan), energy dispersive spectroscopy (EDS), X-ray diffraction (XRD) (X'Pert, Philips, Holland) and Fourier-transform attenuated total reflectance infrared spectroscopy (FTIR) (FT-IR Perkin Elmer GX-X00). Magnetic properties of the samples were measured with a Lakeshore 7307 vibrating sample magnetometer (VSM), in applied fields from −12.5 to 12.5 KOe and 60 Hz in frequency.

Particle size and shape were studied by transmission electron microscopy (TEM) (Titan 80300 Kv). The samples were prepared by placing one drop of the dilute suspension of magnetite nanoparticles in acetone on a carbon coated copper grid and allowing the solvent to evaporate slowly at room temperature.

2.5. Solution analysis

The concentration of Ca, P and Si of the SBF, before and after immersing the magnetite particles, was analyzed by inductively-coupled plasma atomic emission spectrometry (ICP) (IRIS Intrepid II XSP, Thermo Elemental Instruments).

2.6. In vitro hemolysis assay

The hemolysis test was performed using human whole blood from healthy non-smoking donors with permission, following the proper guidelines for studies using human specimens. Blood, collected in heparinized-tubes, was centrifuged at 3000 rpm for 4 min at 4 °C. The obtained pellets were washed three times with cold Alsever's solution (dextrose 0.116 M, NaCl 0.071 M, sodium citrate 0.027 M and citric acid 0.002 M at pH 6.4). The supernatant was then removed and 100 μl of the purified erythrocytes were diluted 1:99 with Alsever's solution. Then, 150 μl of this suspension were again diluted in Alsever's buffer and taken for the curve-response experiments (total volume 2000 μl). This suspension of red blood cells was always freshly prepared and used within 24 h after collection.

Three concentrations of nanoparticles were tested: 0.25, 0.50 and 3.0 mg/ml. Magnetic nanoparticles were brought in direct contact with the blood samples. The tubes were gently mixed in a rotator shaker and then incubated at 37 °C ± 1 °C within a shaking water bath for 30 min. Alsever's solution and deionized water were used as negative (0% hemolysis) and positive (100% hemolysis) controls, respectively. Each group contained three tubes. The specimens were then centrifuged under 3000 rpm for 4 min to collect the supernatant. In order to avoid false-positive results due to nanoparticles absorbance at the assay wavelength, the iron oxide nanoparticles were removed from supernatants using permanent magnets [23].

The absorbance (A) value of the hemoglobin released from the erythrocyte cells was measured spectrophotometrically at 415 nm (Thermospectronic Genesys 5). All trials were performed three times. The hemolysis rate (HR) was calculated as follows: HR (%)=[(A of the experimental group − A of the negative control group)/(A of the positive control group − A of the negative control group)] × 100% [24]. Less than 5% hemolysis was regarded as non-toxic effect level. The experiments were performed in triplicate and were repeated twice to obtain 6 experimental units. The values obtained were expressed as mean ± SD (standard deviation). The data were analyzed with MINITAB 15 software. No a significant difference was considered when $P < 0.05$.

3. Results and discussion

The general aspects and morphology of magnetite nanoparticles and calcium silicate coated nanoparticles are shown in Fig. 1. The magnetite particles are approximately spherical and the mean size was about 8 nm according with the TEM image (Fig. 1A). Fig. 1B shows the TEM image of magnetite after calcium silicate treatment. In a high-resolution transmission electron microscope (HRTEM) micrograph (Fig. 1C) the thin amorphous layer of calcium silicate (~2 nm) is clearly visible on the surface of the magnetite nanoparticles.

Fig. 2 shows the FTIR spectra of the surface of the uncoated magnetite, after calcium silicate treatment and after calcium silicate treatment followed by immersion in SBF for 7 days. Since magnetite has an inverse spinel-type structure, it shows bands indicating the vibrations M_T-O-M_O ($\approx$ 600–550 cm^{-1}), where M_T and M_O correspond to the metal occupying tetrahedral and octahedral positions, respectively, as observed in the spectrum corresponding to the untreated material. The spectrum of the calcium

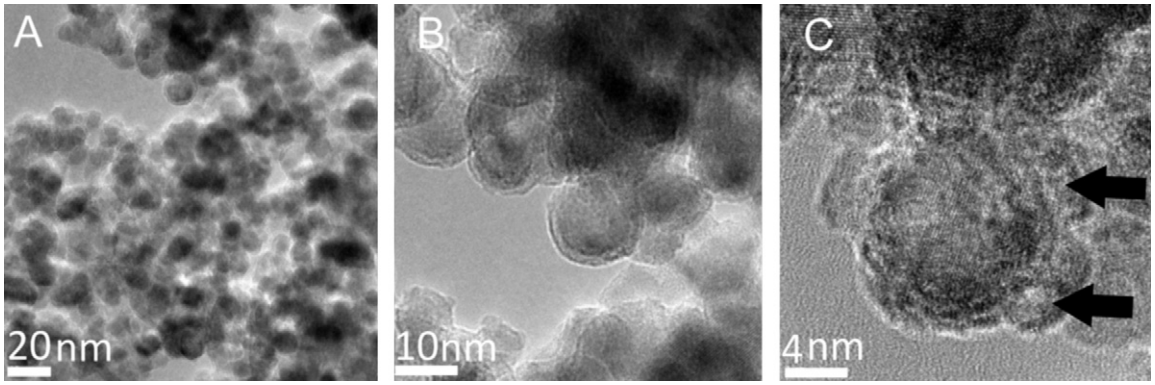

Fig. 1. TEM images of the surfaces of the untreated magnetite nanoparticles (A), the magnetite nanoparticles after the calcium silicate treatment (B) and HRTEM image of the surfaces of magnetite nanoparticles after the calcium silicate treatment (C).

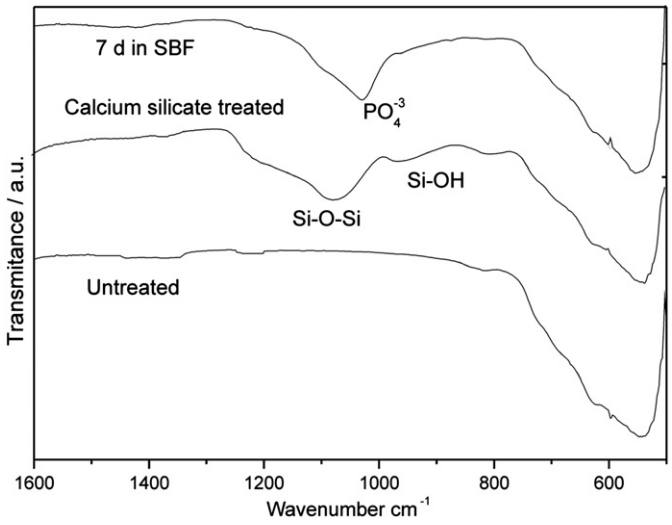

Fig. 2. FTIR spectra of the surfaces of the untreated magnetite nanoparticles, the nanoparticles after treatment with calcium silicate solution and those treated with calcium silicate solution after 7 days of immersion in SBF.

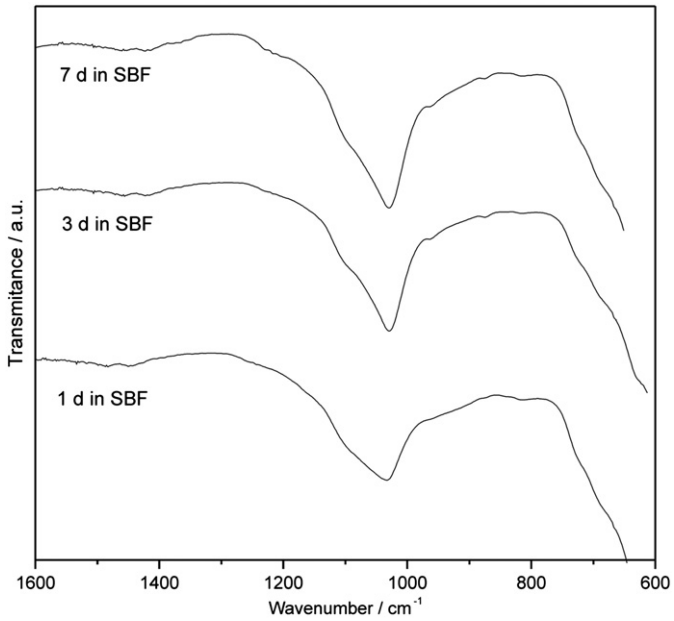

Fig. 3. FTIR spectra of the surfaces of the magnetite nanoparticles after treatment with calcium silicate solution and the magnetite nanoparticles after treatment with calcium silicate solution followed by immersion in SBF for 1, 3 or 7 days.

silicate coated magnetite showed the characteristic absorptions for the silica network located at 1080 and 800 cm^{-1} due to the siloxane groups (Si–O–Si) and a shoulder at 960 cm^{-1} due to the Si–O–H bond vibrations associated to silanol groups [4,25,26]. After immersion in SBF, reflection peaks of the phosphate group (PO_4^{3-}) at 1030 cm^{-1} were observed. These results are in agreement with those reported by Leonor and Baran [20].

As mentioned before, the particles treated with calcium silicate were immersed in SBF for 1, 3 or 7 days. FTIR analysis was performed in order to characterize the chemical structure of the surface of those magnetite nanoparticles.

Fig. 3 shows the FTIR spectra of nanoparticles after 1, 3 and 7 days of immersion. In order to compare the changes occurred before and after immersion in SBF of the calcium silicate treated samples, the spectrum corresponding to the sample after 7 days was also included in Fig. 2. The reflection peak at 1030 cm^{-1} for the phosphate group was observed for all the samples. Comparing the spectra it is possible to observe that as the immersing time in SBF increases, the phosphate band becomes sharper. After only one day of immersion, bands corresponding to the untreated magnetite can be observed. This may indicate that, at this time, the calcium silicate layer partially dissolves into the SBF.

Fig. 4 shows the XRD patterns of the untreated magnetite nanoparticles, the treated with a calcium silicate solution and the treated with a calcium silicate solution followed by immersion in SBF for 7 days. The XRD pattern of the untreated magnetite nanoparticles and that corresponding to the calcium silicate treated exhibit the characteristic peaks of magnetite (JCPDS 19–629). After immersion in SBF of the sample treated with a calcium silicate, new diffraction peaks appeared at 25.8° and 31.7°

2θ corresponding to (002) and (211) diffraction planes of apatite, respectively (JCPDS 9–432) [27,28].

Fig. 5 shows the surface of the magnetite nanoparticles treated with calcium silicate solution (Fig. 5A), and then immersed in SBF for 1, 3 and 7 days (Fig. 5B, C and D, respectively). After immersion in the calcium silicate solution, the nanoparticles were agglomerated (Fig. 5A). When the magnetite nanoparticles treated with calcium solution were immersed in SBF for 1 day (Fig. 5B), a Ca, P-rich layer was formed on the surface of the agglomerates as demonstrated by the corresponding EDS spectrum. This layer became denser by increasing immersing time in SBF (Fig. 5C and D). According to the XRD results showed earlier, this Ca, P-rich compound corresponds to apatite.

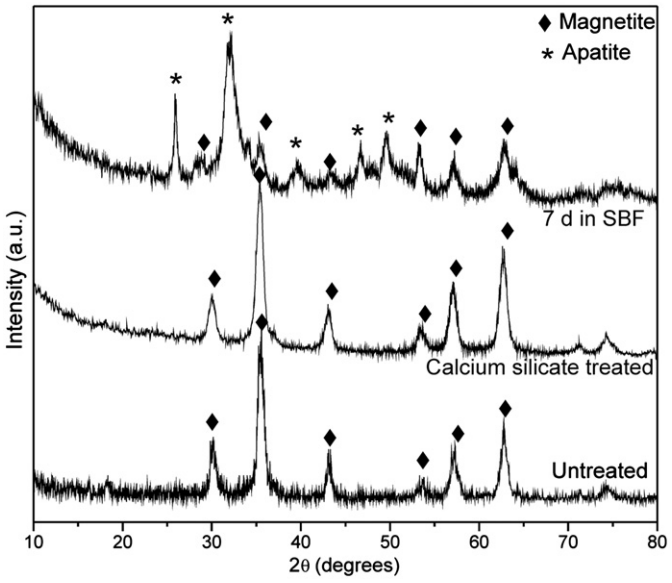

Fig. 4. XRD patterns of the untreated magnetite nanoparticles, the nanoparticles after calcium silicate treatment and the magnetite nanoparticles after treatment with calcium silicate solution followed by immersion in SBF for 7 day.

By EDS analysis the presence of silicon (Si), chlorine (Cl) and calcium (Ca) was detected on the surface of the magnetite nanoparticles which is in agreement with the calcium silicate treatment. After immersion in SBF, Ca and P peaks were detected. The intensity of the Ca and P peaks increased significantly as immersing time in SBF was increased. These results are in good agreement with those obtained from the FTIR analysis shown in Fig. 3. The Ca/P ratio of the layer formed after 7 days in SBF was evaluated from the EDS analysis. The mean value of five analyses performed in different particles was 1.65±0.06, which is close to that corresponding to hydroxyapatite (1.67).

The hysteresis loops of magnetite nanoparticles are shown in Fig. 6. The saturation magnetization (M_s) of the untreated magnetite nanoparticles was 48.6 emu/g, which is in agreement with the reported value [29]. For the calcium silicate treated magnetite M_s was 38.8 emu/g,

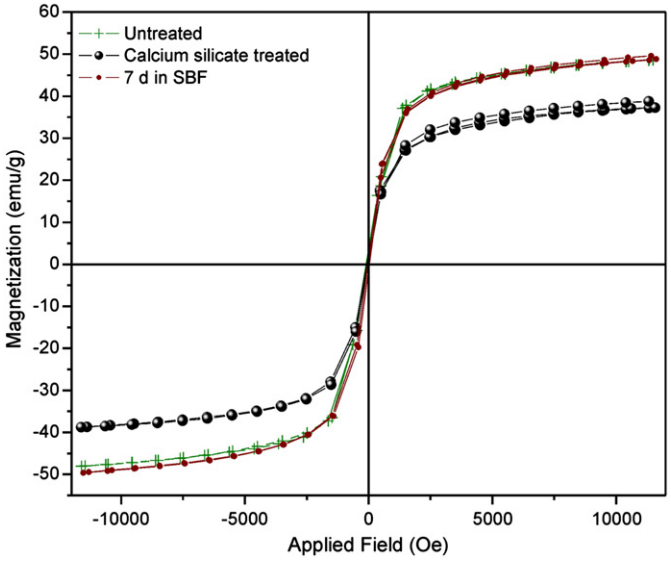

Fig. 6. Hysteresis loops of magnetite nanoparticles: (A) untreated, (B) after calcium silicate treatment and (C) after calcium silicate treatment followed by immersion in SBF for 7 days.

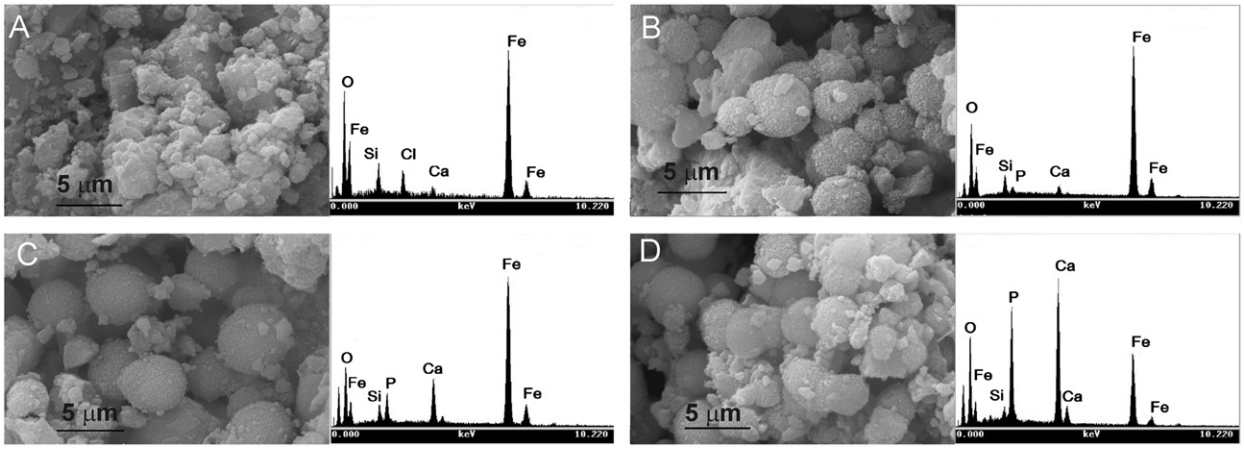

Fig. 5. SEM images and EDS spectra of the magnetite nanoparticles treated with a calcium silicate solution (A) and the nanoparticles treated with a calcium silicate solution followed by their immersion in SBF for 1 (B), 3 (C) or 7 days (D).

this may be due to the mass proportion of the magnetite nanoparticles. After 7 days of immersion of this sample in SBF, M_s was increased up to 49.6 emu/g. These results indicate the dissolution of the calcium silicate gel into the SBF, as shown in the ICP results (Fig. 7).

Fig. 7 shows the changes in Ca, P and Si concentrations in SBF. The ICP results indicated that at the beginning of immersion (day 1), the concentration of Ca was increased when the sample was treated with calcium silicate. This may be due to the release of calcium ions from the surface of the nanoparticles into the SBF. After this period of time, the Ca concentration decreased. This decrease may be due to the nucleation of the Ca, P- rich layer on the calcium silicate treated magnetite. The P concentration in SBF was also decreasing. This is due to the interaction with the calcium in the solution and the formation of apatite. The release of silicon is attributed to the partial dissolution of the calcium silicate layer, which results in the formation of the Si–OH groups that are responsible for the apatite nucleation [20]. In order to compare the ion concentration changes in SBF, in this Fig. 7 the changes in Ca, P and Si after immersing the untreated magnetite sample were also included. These behaviors indicate that the calcium silicate treatment improves the apatite formation ability.

In a previous report we found that it is possible to form an apatite layer when the magnetite nanoparticles were immersed in SBF using a reimmersion method and a wollastonite disk [19]. In this work, we have found that it is possible to reduce the immersion time if the magnetite nanoparticles are treated previously in a calcium silicate solution. The formation of Si–OH groups may be possible due to the release of the calcium ions (Ca^{2+}) of the calcium silicate into the SBF via ionic exchange with the hydronium ion (H_3O^+). These groups on the surface of the magnetite induce apatite nucleation. The released Ca^{2+} accelerates apatite nucleation by increasing the ionic activity product of the apatite in the SBF. Once the apatite nuclei are formed, they can grow forming a uniform layer by consuming calcium and phosphate ions from the SBF, since the SBF is already highly supersaturated with respect to apatite [30,31]. Leonor and cols. [20] suggested that some chemical bondings, such as Si–O–Ca–O–Si, exist at the interface between apatite and calcium silicate.

The results of the hemolytic test (Fig. 8) demonstrated that the HRs of the samples were lower than 2%. This finding indicates that the untreated magnetite nanoparticles, the magnetite nanoparticles treated with calcium silicate and the magnetite nanoparticles treated with calcium silicate followed by immersion in SBF for 7 day had no hemolytic reaction at all tested concentrations up to 3.0 mg/ml. According to ASTM F 756–08 (Standard Practice for Assessment of Hemolytic Properties of Materials) [24], a HR < 2% produced by any material could be considered as not hemolytic.

Consequently, we can assume that all these samples are compatible with erythrocytes when they are circulating in the human blood and it was consistent with the requirement of hemolytic test for biomaterials [32]. The obtained results also indicate that the untreated magnetite nanoparticles and the magnetite nanoparticles treated with calcium silicate exhibited a high degree of hemolytic activity at 3.0 mg/ml as compared with the SBF treatment. Therefore, it seems that the apatite coating adds a protective effect from the hemolysis, since hemolysis of magnetite treated with calcium silicate is higher than that corresponding to the sample after immersion in SBF. No significant differences were found in hemolysis levels among all groups ($P < 0.05$).

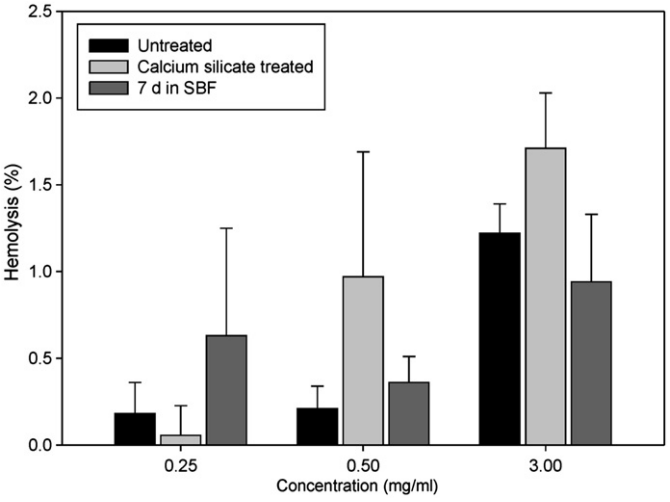

Fig. 8. Hemolysis caused by different magnetite nanoparticles.

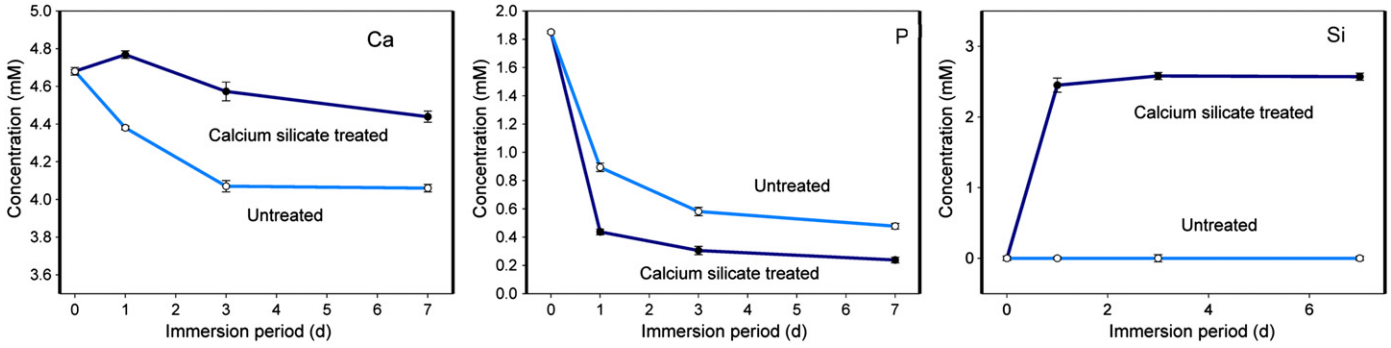

Fig. 7. ICP results of Ca, P and Si concentrations in SBF.

Due to the superparamagnetic behavior at room temperature and non hemolytic activity, well-dispersed nanoparticles in a carrier medium can be injected and transported to the tissue through blood vessels under an external applied magnetic field. Furthermore, due to the bioactivity of these magnetite particles, they are expected to bond chemically to bone, leading to the feasibility to repeat the hyperthermia treatments at different periods of time.

4. Conclusions

The magnetite nanoparticles treated with a calcium silicate solution can be coated with a bonelike apatite layer after only one day of biomimetic treatment using SBF. These bioactive ferrite particles showed also a superparamagnetic behavior and non hemolytic activity. Thus, these magnetite nanoparticles can be successfully used as thermoseeds for hyperthermic treatment of solid bone tumors under an alternating magnetic field.

Acknowledgments

E.M. Múzquiz Ramos thanks CONACyT-Mexico for the financial support (scholarship 219709). The authors also thank M.A. Aguilar González for his valuable technical and professional assistance.

References

[1] A. Ito, M. Shinkai, H Honda, T. Kobayashi, Medical applications of functionalized magnetic nanoparticles, Journal of Bioscience and Bioengineering 100 (2005) 1–11.
[2] A.K. Gupta, M. Gupta, Synthesis and surface engineering of iron oxide nanoparticles for biomedical applications, Biomaterials 26 (2005) 3995–4021.
[3] O. Bretcanu, E. Verné, M. Cöisson, P. Tiberto, P. Allia, Temperature effect on the magnetic properties of the coprecipitation derived ferrimagnetic glass-ceramics, Journal of Magnetism and Magnetic Materials 300 (2006) 412–417.
[4] D.M. Souza, A.L. Andrade, J.D. Fabris, P. Valerio, A.M. Goes, M.F. Leite, R.Z. Domingues, Synthesis and in vitro evaluation of toxicity of silica-coated magnetite nanoparticles, Journal of Non-Crystalline Solids 354 (2008) 4894–4897.
[5] K. Kim, E. Kim, J. Lee, S. Maeng, Y. Kim, Synthesis and characterization of magnetite nanopowders, Current Applied Physics 8 (2008) 758–760.
[6] A. del Campo, T. Sen, J.P. Lellouche, I.J. Bruce, Multifunctional magnetite and silica–magnetite nanoparticles: Synthesis, surface activation and applications in life sciences, Journal of Magnetism and Magnetic Materials 293 (2005) 33–40.
[7] R.V. Ramanujan, Clinical Applications of Magnetic Nanomaterials, in: F.K. Fuss, S.L. Chia, S.S. Venkatraman, S.M. Krishnan, B. Schmidt (Eds.), Proc. First Intl. Bioengg. Conf, Singapore, 2004, p. 174.
[8] M. Kawashita, M Tanaka, T Kokubo, Y. Inoue, T. Yao, S. Hamada, T. Shinjo, Preparation of ferrimagnetic magnetite microspheres for in situ hyperthermic treatment of cancer, Biomaterials 26 (2005) 2231–2238.
[9] D.H. Kim, S.H. Lee, K. Kim, K.M. Kim, I.B. Shim, Y.K. Lee, Cytotoxicity of ferrite particles by MTT and agar diffusion methods for hyperthermic application, Journal of Magnetism and Magnetic Materials 293 (2005) 287–292.
[10] S. Ĉampelj, D. Makovec, M. Drofenik, Functionalization of magnetic nanoparticles with 3-aminopropyl silane, Journal of Magnetism and Magnetic Materials 321 (2009) 1346–1350.
[11] M.L. Vadala, M.A. Zalich, D.B. Fulks, T.G. Pierre St., J.P. Dailey, J.S. Riffle, Cobalt–silica magnetic nanoparticles with functional surfaces, Journal of Magnetism and Magnetic Materials 293 (2005) 162–170.
[12] A. Nogiwa, D.A. Cortés, Bone-like apatite coating on Mg-PSZ/Al_2O_3 composites using bioactive systems, Journal of Materials Science Materials in Medicine 17 (2006) 1139–1144.
[13] D.A. Cortés, A.A. Nogiwa, J.M. Almanza, S. Ortega, Biomimetic apatite coating on Mg-PSZ/Al_2O_3 composites. Effect of the immersion method, Materials Letters 59 (2005) 1352–1355.
[14] D.A. Cortés, A. Medina, J.C. Escobedo, S. Escobedo, M.A. López, Effect of wollastonite ceramics and bioactive glass on the formation of a bonelike apatite layer on a cobalt base alloy, Journal of Biomedical Materials Research Part A 70 (2004) 341–346.
[15] I.B. Leonor, E.T. Baran, M. Kawashita, R.L. Reis, T. Kokubo, T. Nakamur, Growth of a bonelike apatite on chitosan microparticles after a calcium silicate treatment, Acta biomaterialia 4 (2008) 1349–1359.
[16] Y. Abe, T. Kokubo, T. Yamamuro, Apatite coating on ceramics, metals and polymers utilizing a biological process, Journal of Materials Science Materials in Medicine 1 (1990) 233–238.
[17] P.N. De Aza, Z. Luklinska, M. Anseau, F. Guitian, S. De Aza, Bioactivity of pseudowollastonite in human saliva, Journal of Dentistry 27 (1999) 107–113.
[18] P.N. De Aza, F. Guitian, S. De Aza, Bioactivity of wollastonite ceramics: In vitro evaluation, Scripta Metallugica et Materialia 31 (1994) 1001–1005.
[19] E.M. Múzquiz, D.A. Cortés, J. Escobedo, Biomimetic apatite coating on magnetite particles, Materials Letters 64 (2010) 1117–1119.
[20] I.B. Leonor, E.T. Baran, M. Kawashita, R.L. Reis, T. Kokubo, T. Nakamura, Growth of a bonelike apatite on chitosan microparticles after a calcium silicate treatment, Acta Biomaterialia 4 (2008) 1349–1359.
[21] R. Betancourt, O. Ayala, L.A. García, O. Rodríguez, J. Matutes, G. Ramos, H. Yee, Synthesis and magneto-structural study of $Co_xFe_{3-x}O_4$ nanoparticles, Journal of Magnetism and Magnetic Materials 294 (2005) 33–36.
[22] T. Kokubo, H. Kushitani, S. Sakka, Solutions able to reproduce in vivo surface-structure changes in bioactive glass-ceramic A-W, Journal of Biomaterials Research 24 (1990) 721–734.
[23] NCL Method ITA-1. Analysis of Hemolytic Properties of Nanoparticles. Nanotechnology Characterization Laboratory. National Cancer Institute-Frederick. 2009. 〈http://ncl.cancer.gov/NCL_Method_ITA-1.pdf〉. Last accessed: 27/IV/2011.
[24] ASTM F-756, Standard Practice for Assessment of Hemolytic Properties of Materials, 2009, Annual Book of ASTM Standars. Committee F04 Medical and Surgical Materials and Devices, Subcommittee F04.16 Biocompatibility Test Methods.
[25] S. Zhang, D. Dong, Y. Sui, Z. Liu, H. Wang, Z. Qian, W. Su, Preparation of core shell particles consisting of cobalt ferrite and silica by sol–gel process, Journal of Alloys and Compounds 415 (2006) 257–260.
[26] X.H. Huang, Z.H. Chen, Sol–gel preparation and characterization of $CoFe_2O_4$–SiO_2 Nanocomposites, Solid State Communications 132 (2004) 845–850.
[27] M. Okuda, M. Takeguchi, O. Ruairc, M Tagaya, Y Zhu, A. Hashimoto, N. Hanagata, W. Schmitt, T. Ikoma, Structural analysis of hydroxyapatite coating on magnetite nanoparticles using energy filter imaging and electron tomography, Journal of Electron Microscopy 59 (2010) 173–179.
[28] A. Martınez, I. Izquierdo, M. Vallet, Bioactivity of a CaO-SiO_2 Binary Glasses System, Chemistry of Materials: a Publication of the American Chemical Society 12 (2000) 3080–3088.

[29] Y. Sun, L. Duan, Z. Guo, Y. Duan, M. Ma, L. Xu, Y. Zhang, N. Gu, An improved way to prepare superparamagnetic magnetite-silica core-shell nanoparticles for possible biological application, Journal of Magnetism and Magnetic Materials 285 (2005) 65–70.

[30] T. Kokubo T, H.M. Kim, M. Kawashita, Ceramics for biomedical applications, in: S. Somiya, F. Aldinger, N. Claussen, R.M. Spriggs, K. Uchino, K. Kuomoto et al.(Eds.), Handbook of Advanced Ceramics, Vol II Processing and their applications, Elsevier Academic Press, Oxford, 2003, p. 396.

[31] X. Liua, C. Dinga, P.K. Chu, Mechanism of apatite formation on wollastonite coatings in simulated body fluids, Biomaterials 25 (2004) 1755–1761.

[32] Z.Y. Wang, J Song, D.S. Zhang, Nanosized As_2O_3/Fe_2O_3 complexes combined with magnetic fluid hyperthermia selectively target liver cancer cells, World Journal of Gastroenterology 15 (2009) 2995–3002.